Deuterium occupation of tetrahedral sites in palladium

K. G. McLennan,*,† E. MacA. Gray, and J. F. Dobson
Nanoscale Science and Technology Centre, Griffith University, Brisbane 4111, Australia
(Received 10 September 2007; revised manuscript received 23 April 2008; published 9 July 2008)

The long-standing controversy over the occupation by hydrogen of tetrahedral interstices in palladium has been addressed experimentally and theoretically. Using the highest resolution neutron powder diffractometer available, diffraction profiles were recorded from single-phase samples obtained by loading Pd with deuterium *in situ* at 310 °C, at D_2 pressures up to 90 bar. Rietveld profile analysis showed that a model including tetrahedral occupancy was necessary to properly fit the experimental diffraction profiles. The maximum absolute tetrahedral occupancy was found at a deuterium-to-metal atomic ratio of 0.6, where about one-third of all *D* atoms were in tetrahedral sites. At the lowest and highest *D* concentration, the tetrahedral fraction approached zero. The energy of formation was calculated, based on density-functional theory, for numerous configurations of octahedral and tetrahedral interstitials in a supercell, which modeled stoichiometries Pd_8H_n such that $n=1,2,\ldots 8$. For Pd_8H_3, the minimum formation energy was found with 1–2 tetrahedral atoms. For all other stoichiometries, the minimum formation energy was 0–1 tetrahedral atoms. Thus, the calculations are in excellent qualitative agreement with experiment and support the reality of tetrahedral occupancy.

DOI: 10.1103/PhysRevB.78.014104 PACS number(s): 61.50.Ks, 61.05.fm, 71.20.Be

I. INTRODUCTION

Palladium is the best-known metallic absorber of hydrogen.[1] When it is exposed to hydrogen gas at suitable temperature and pressure, the hydrogen molecule dissociates at the Pd surface and hydrogen atoms are chemisorbed, diffusing into the metal via interstices in the metal crystal lattice and occupy these interstices up to a hydrogen-to-metal atomic ratio, H/M, approaching one at high pressure and low temperature.[2] As the hydrogen pressure over the metal increases, the dilute solid-solution phase (α) becomes unstable and the concentrated hydride phase (β) forms. Ordering of hydrogen in the β phase occurs at cryogenic temperatures. This miscibility-gap system has a thermodynamic critical point that is reported to be at 283 °C and 39 bar D_2 pressure.[3] The supercritical phase may be best described as concentrated α.

There are two interstitial sites in the fcc Pd lattice: the octahedral (*O*) site at (0,0,0), $(\frac{1}{2},\frac{1}{2},0)$ …, and the tetrahedral (*T*) site at $(\frac{1}{4},\frac{1}{4},\frac{1}{4})$, $(\frac{1}{4},\frac{1}{4},\frac{3}{4})$ …, relative to the center of the Pd unit cell. The equilibrium site occupancy has been a long-standing controversy, with the prevailing view being that only the *O* site is occupied. The latest experimental work,[4] however, produced diffraction evidence that the *T* site is partially occupied when the deuteride PdD_x is formed above the thermodynamic critical point.

The earliest diffraction with x rays[5] confirmed the existence of the α and β phases and that these phases retain the basic structure of the metal. *In situ* x-ray diffraction also revealed the single-phase nature of palladium hydride above the thermodynamic critical point.[6] These experiments could not give information about interstitial site occupancy owing to the insensitivity of x-ray diffraction to the low charge density of hydrogen.

The first neutron diffraction experiment,[7] on $PdH_{0.71}$ and $PdD_{0.66}$, concluded that both *H* and *D* occupied octahedral positions only. The first single-crystal neutron-diffraction study[8] did not consider tetrahedral occupation in the $PdH_{0.63}$ sample, but did confirm that the method of loading the hydrogen, from the gas phase or electrochemically, produced no structural differences.

The reader is referred to the previous paper[4] from this group for a brief critical review of the most relevant of the numerous neutron-diffraction studies[7–25] that have been made by both diffraction and inelastic neutron techniques. The consensus has been that the *O* site only is occupied, with evidence for *T*-site occupancy being regarded as controversial. With one exception,[10] only models based on *O*-only or *T*-only occupancy were considered in the reported data analyses.

Given that the diffusion of hydrogen through palladium occurs by interstitial hopping of the hydrogen from *O* site to *O* site via *T* sites, occupancy becomes an issue of residence time. A series of theoretical papers by Elsässer and co-workers,[26–31] reporting first-principles total-energy calculations of vibration states of hydrogen isotopes in stoichiometric PdH and (hypothetical) PdH_4, sheds considerable light here. The *T*-site potential energy was found to be a little higher than that of the *O* site, but allowing the surrounding Pd atoms to relax led to a very significant self-trapping effect in which the *T*-site potential energy was lowered until it was essentially equal to the *O*-site energy in PdH. The height of the saddle separating the *O* and *T* sites in the ⟨111⟩ direction fell from 300–500 meV to 150–200 meV when fully relaxed.[31] The accepted activation energy for dilute *H* diffusing in Pd (230 meV) corresponds to this energy range when added to its zero-point vibration energy in the *O* site, suggesting that the predicted relaxed *T*-site energy is reasonable and that, therefore, substantial *T*-site residence is thermodynamically feasible.

It was found[27] that the zero-point vibration energy of the *H* isotope in the rather small *T* site was comparable to the activation potential energy to the adjacent *O* sites via the ⟨111⟩ saddles, meaning that this state would not be very stably occupied. In the case of the *D* isotope, however, its higher mass led to a zero-point energy less than the activation potential energy to jump from a *T* site, thus raising the

possibility of stable *T*-site occupancy. Further work by the same group[31] suggests that there are in fact real bound states for all hydrogen isotopes at the *T* sites, but only virtual bound states for muons and pions, which are much lighter than *H*.

For the work reported here, a combined experimental and theoretical approach was taken. In view of the controversy surrounding interstitial occupancy by hydrogen in Pd, neutron powder-diffraction measurements were made on two diffractometers that work on different principles, one fixed wavelength, the other time of flight. The experimental conditions facilitated comparison with theoretical calculations of the energetics of the Pd-hydrogen system. Principally, this meant loading Pd with deuterium *in situ* at temperatures and pressures where the system is single-phase and able to be modeled by pseudostoichiometries such as Pd_4D. Calculations of the formation energies of several pseudostoichiometries were performed with the ADF BAND software,[32] which uses a density-functional-theory (DFT) approach.

II. METHODS

A. Experiment

Independent knowledge of the global *D* content of the sample is of primary importance in crystallography-based studies of hydrogen in materials, as it may be used to decide between alternative structural models which are found to fit the diffraction profile with equivalent quality-of-fit indices, based on the fitted *D* occupancies.

1. Determining global hydrogen concentration

The Sieverts technique was used for this study. This involves establishing a pressure of hydrogen gas in an accurately known reference volume, admitting this gas to the sample cell, and determining the amount absorbed by the sample from the change in the pressure in the system. As the calculation of the quantity of absorbed hydrogen involves taking differences between the amounts of hydrogen gas present before and after absorption, where the absorbed amount may be rather small compared to the amount of gas in the system, it is vital to calculate as accurately as possible the number of moles of gas present under the experimental conditions of temperature and pressure. Accurate knowledge of the compressibility, *Z*, defined by $pV_m/RT=Z$ rather than 1 as in the ideal case, is essential. For this work, a recently developed expression for deuterium gas[38] was used to obtain compressibility values with accuracy better than $\pm 0.1\%$. The temperatures of the gas in the hydrogenator manifold and the sample cell were measured by platinum thermometers attached to the outside of the volume and isolated from the surroundings with insulation, with respective accuracies ± 0.1 and ± 1.0 °C. The deuterium pressure was measured with an accuracy of ± 7 kPa in the experimental pressure range of 0–10 MPa. The estimated accuracy with which the D/M atomic ratio was determined was ± 0.01.

2. Determination of interstitial site occupancies

Neutron powder-diffraction patterns were collected on two instruments, the time-of-flight (TOF) HRPD[36] instrument at the ISIS neutron spallation source, U.K., and the fixed-wavelength HRPD[37] instrument at the HIFAR reactor source, Australia. In every case, deuterium was loaded into the sample *in situ* and the D/M ratio of the sample was measured throughout the experiment, as detailed in §*II.A.2*. Data from the backscattering detector bank of HRPD(ISIS) were used for this work. The instrumental resolution in *d*-spacing is approximately $\Delta d/d=4\times10^{-4}$, which is the highest of any current neutron powder diffractometer. HRPD(HIFAR) was operated at a wavelength of 1.88504 Å and data were recorded at 2θ intervals of 0.05°.

The basis for distinguishing *O*-site and *T*-site occupation is crucial to the experimental analysis and is therefore explained in some detail here. The *O* sites in Pd lie on a fcc sublattice, so the stoichiometric deuteride, PdD, would have the NaCl structure. The similarity of the neutron-scattering lengths of deuterium (6.674 fm) and palladium (5.91 fm)[33] means that perfectly octahedral PdD would be almost simple cubic with a halved lattice parameter compared to Pd, so $(111)_{Pd}$ would be nearly quenched. Hence *D* addition in *O* sites lowers the (111) reflection strongly, as observed experimentally.[7] In contrast, the *T* sites lie in (200) planes and therefore contribute significantly to the (200) and (220) reflections, but not to (111). Thus, the effects of adding *D* in *O* or in *T* sites are in principle easy to distinguish in PdD_x.

Using the structure factor rules for the $Fm3m$ space group,[34] the real and imaginary parts of the structure factor for the (hkl) reflection are

$$A = 32\cos^2 2\pi\frac{h+k}{4}\cos^2 2\pi\frac{k+l}{4}\{\cos 2\pi hx[\cos 2\pi ky\cos 2\pi lz+\cos 2\pi ly\cos 2\pi kz]$$
$$+\cos 2\pi hy[\cos 2\pi kz\cos 2\pi lx+\cos 2\pi lz\cos 2\pi kx]+\cos 2\pi hz[\cos 2\pi kx\cos 2\pi ly+\cos 2\pi lx\cos 2\pi ky]\},$$
$$B = 0 \qquad (1)$$

where the atom position (x,y,z) is relative to the center of the unit cell. Table I shows the predicted effects on the integrated intensities of some low-order peaks of adding an equal amount of an interstitial element with scattering length equal to that of the host material to either the *O* or the *T* site, confirming the conclusions based on intuition. As Bragg intensity depends on the square of the scattering length, the error in assuming equal scattering lengths is quite small.

The key to the measurement of *O*-site and *T*-site occupancies by diffraction is therefore the use of an analysis tech-

TABLE I. Effects on low-order peak intensities of adding one interstitial atoms per Pd atom, with the same scattering length as Pd, in *O* or *T* sites. *A* is the real part of the structure factor (see text).

Bragg peak	*A* (Pd)	Octahedral site (change in *A*)	Tetrahedral site (change in *A*)
(111)	768	Decrease (−768)	No effect (0)
(200)	768	Increase (+768)	Decrease (−1536)
(220)	768	Increase (+768)	Increase (+1536)

nique that fits the entire diffraction profile. Rietveld profile refinement was appropriate for the powdered polycrystalline sample used in this study. The Rietica computer code[35] was used for all refinements. Figure 1 illustrates the expected variation in low-order peak heights for varying *D* occupancy of only *O* sites, using the actual scattering lengths for Pd and *D*, obtained by calculating model diffraction patterns in Rietica, for both of the diffractometers used in this study, using real instrument parameters to model the effects of instrument

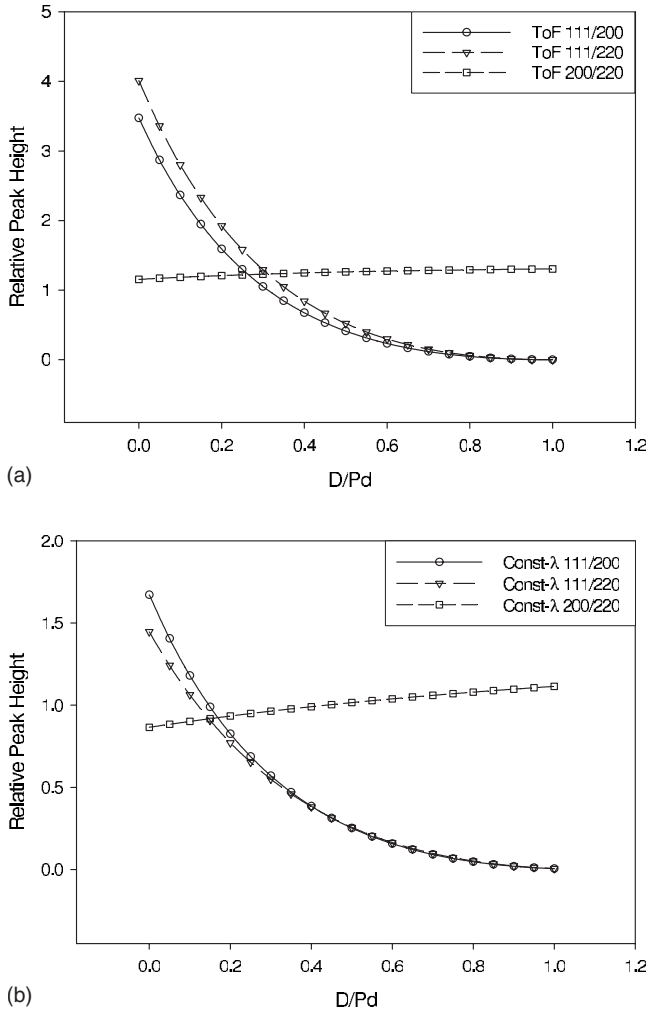

FIG. 1. Calculated low-order peak height ratios for octahedral PdD_x on (a) a time-of-flight (HRPD at ISIS) and (b) a fixed-wavelength (HRPD at HIFAR) neutron powder diffractometers.

optics. The TOF instrument's higher resolution and its constancy with *d* spacing are the cause of the stronger dependence of the (111)/(220) peak height ratio in this case.

Based on an independent determination of the global *D* content of the sample (see Sec. II A 2), the following procedure was used to adjust both the *O* and *T* occupancies systematically during Rietveld refinement. A Le Bail fit (independent peak intensities) was used for the peaks from the stainless-steel sample cell, which exhibited very strong preferred orientation. The PdD_x structure was modeled in the $Fm3m$ space group. The thermal parameters of the *D* interstitials were constrained such that the octahedral site thermal parameter was 3.4 times the tetrahedral site thermal parameter, i.e., the square of the ratio of the octahedral and tetrahedral interstitial hole sizes.

First, the lattice parameter was refined. Next, the *D* occupancy of the *O* site was refined with no *D* permitted on the *T* site, until the best fit was achieved to the intensity of (111). The corresponding value of D/M was then calculated as described in Sec. II A 2 and compared to the manometric determination. The balance of the *D* occupancy was then assigned to the *T* site. Then lattice parameter, scale factor, background, thermal parameters, preferred orientation, and sample dependent peak-shape parameters were refined separately. We then returned to refine the *O* occupancy only, paying attention primarily to the height of the (111) peak, and repeated the process until a stable fit to the overall pattern was achieved, ensuring that any singly refined parameter improved the goodness-of-fit indices.

3. Sample preparation and environment

Pd powder from Goodfellow Metals with initial particle sizes in the range of 45–400 μm was used. This was the same sample used in previous work by this group.[4,23–25] The sample was exposed *in situ* to 30 kPa of hydrogen at a sample temperature of 500 °C to help reduce any oxide layers on the particle surfaces and then annealed at 500 °C (roughly the Pd recovery temperature) for 12 h under vacuum in order to anneal the dislocations generated by previous absorption-desorption cycling below the critical temperature. The sample was contained in a stainless-steel cell with inner diameter 10.0 mm and wall thickness 0.75 mm, heated by a vanadium-element furnace under vacuum. Diffraction profiles were recorded at 301–305 °C [HRPD(HIFAR)] and later at 310 °C [HRPD(ISIS)], with an estimated accuracy in temperature readings of ±1 °C. This increase in temperature was mandated by our discovery that the sample passed below the critical point at 305 °C.

A summary of the temperature profiles followed on each diffractometer is presented in Table II.

B. Theory

1. Energetics and structural considerations

Calculations of the formation energy of the palladium-hydrogen system in the pericritical region were performed with the ADF-BAND[32] software, based on DFT in the local density approximation. Note that while absolute atomization

TABLE II. Summary of sample temperatures and diffraction instruments used to collect patterns.

Instrument	Temperature profiles	
HRPD(HIFAR)	25 °C	301–306 °C
MRPD(HIFAR)		309 °C
HRPD(ISIS)	25 °C	310 °C

(formation) energies might be improved substantially by going beyond the local density approximation for the exchange-correlation energy, the energies of interest here are differences taken between similar configurations of the ions, involving relatively minor changes in the electronic orbitals. For such cases (in contrast to the case of atomization where orbital characters are greatly altered), experience suggests that the LDA will be rather good. Indeed, the formation energies used here were only an intermediate step, and the energy of the fully atomized configuration that appear implicitly in these formation energies actually cancels out when one forms the differences of formation energies between different solid configurations, as was done here.

As we used a zero-temperature LDA technique, the isotopic identity of the interstitial is not accounted for. The experimental temperatures were well below 1000 K and thus small compared to the Fermi temperature.

The calculations were performed for a range of pseudostoichiometries Pd_nH_m: Pd, Pd_8H, Pd_4H, Pd_8H_3, Pd_2H, Pd_8H_5, Pd_4H_3, Pd_8H_7, and PdH, corresponding to hydrogen-to-metal atomic ratios 0, 0.125, 0.25, 0.375, 0.5, 0.625, 0.75, 0.875, and 1.0. As the diffraction patterns were recorded above the critical point, where the sample is single phase, the results of the structural analysis were then able to be validly compared to these calculations.

The modeled interstitial concentrations were realized in three unit cells, generally adopting the cell of highest symmetry. For Pd and PdH, a primitive (rhombohedral) fcc cell was used and required least computing resources owing to its highest-possible symmetry. A conventional (cubic) fcc cell permitted Pd, Pd_4H, Pd_2H (as Pd_4H_2), Pd_4H_3 and PdH (as Pd_4H_4) to be modeled. A doubled unit cell can be used to generate Pd_8H_n $(n=0,1,2,\ldots,8)$, again using the highest-symmetry cell according to needs.

In reality, hydrogen randomly occupies the interstitial sites at temperatures of concern in this study, with ordering occurring only below about 100 K. Given the relatively small unit cells capable of calculation using ADF-BAND, a pseudorandom configuration was created for the doubled unit cell whereby for increasing hydrogen content each successively added hydrogen atom was placed into a different subcell than the previous one. The octahedral sites were also "paired" in constructing each octahedral-only configuration. When increasing the hydrogen concentration, every second hydrogen atom was added to the rightmost subcell of the doubled unit cell in the same *O* site as the previous hydrogen atom was placed in the leftmost subcell. Thus, Pd_8H had its hydrogen atom located at the $(a_1/4, a_2/2, a_3/2)$ *O* site (relative to a cell vertex, $a_1=2a$, $a_2=a_3=a$, a=lattice parameter of conventional fcc cell); in Pd_8H_2, two atoms were located at *O* sites $(a_1/4, a_2/2, a_3/2)$ and $(3a_1/4, a_2/2, a_3/2)$ and so on, with a new *O* site added for each pair of new increased concentrations.

Where lattice relaxation was allowed, the following procedure was applied to each configuration of interstitial occupancy. Using the same electronic starting configuration for each structure, the total formation energy was calculated for a range of lattice parameters about the experimentally determined (or interpolated) value. The formation energy was calculated as the difference in energy between the starting electronic configuration for a collection of separate atoms and the final configuration as defined by that collection of atoms in the arrangement provided as input to the ADF-BAND program. These results were then plotted, and a 2nd order polynomial was fitted to the region around the estimated minimum. The minimum of this polynomial was then taken as the minimum-energy lattice parameter.

2. Orbital functions

The electronic configuration of the palladium atoms impacts strongly on the width and position of the *d* band.[39] This fact, along with the enormous number of calculations required to cover all realistic hydrogen concentrations in palladium-hydride, led us to consider only *relative* band-structure changes, based on a free-atom palladium electronic structure of $4d^{10}$. It is also widely accepted[40] that, although the LDA can accurately predict lattice parameters (nevertheless often underestimating metallic elements by the order of 1%), DFT largely fails to accurately calculate absolute energy values, especially when applied to *d*-band metals. The basis functions chosen for the palladium atoms were a mixture of spherically-symmetric numerical (Herman-Skillman-type) functions for the occupied electronic states, Slater-type orbitals for the valence electronic states, and fit-functions for available states.

The calculations were spin unrestricted and spin-orbit coupling was ignored. The Pd subshells were frozen (were not perturbed) up to and including 3*s*, but all states above this, as well as the single *H* electron, were used for the calculations. As numeric orbitals are spherically symmetric, the squares of all *s*, *p*, and *d* orbitals were used as fitting functions with $l=0$. The minimum and maximum range of atomic radii employed were 10^{-6} up to 100 a.u., using 2000 grid points. The local spin-density expression of Vosko, Wilk, and Nusair was used to estimate exchange and correlation.

III. RESULTS AND DISCUSSION

A. Lattice parameters

Figure 2 compares the lattice parameters measured on the same sample using two neutron powder diffractometers, at slightly different temperatures, as noted on the figure. These are the most basic and reliable crystallographic data obtainable by diffraction. Figure 2 reveals that the sample became two phase in the middle range of *D* concentrations, meaning that the isotherm was traversed slightly beneath the critical point. This was surprising and indicates that the accepted critical temperature of the Pd-D_2 system (283 °C)[3] is too

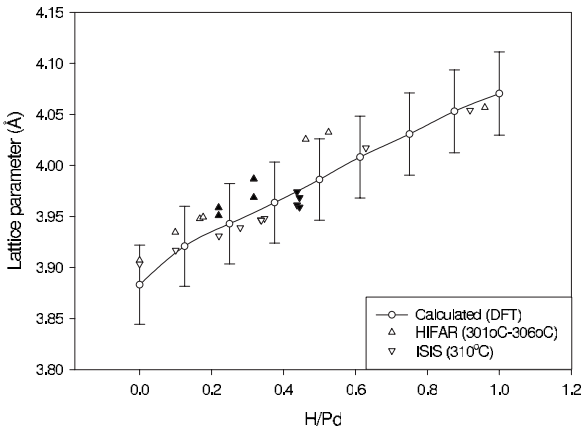

FIG. 2. Comparison of calculated (*O*-only occupancy) and experimental lattice parameters. Filled symbols are two phase, unfilled symbols are single-phase. The two experimental points with the highest D/M values were obtained at room temperature, following quenching through the pure β-phase region.

low. At $D/M \approx 0.43$, the splitting of the diffraction profile into doublets belonging to distinguishable α and β phases was just discernible by eye on HRPD (ISIS) in the backscattering detector bank, and so would not be readily resolved on an instrument with lower resolution. This indicates that the isotherm passed very close to the true critical point of our sample.

Given that the experimental values of the lattice parameter of pure Pd determined using the two diffractometers are in good agreement ($D/M=0$ in Fig. 2), the discrepancies between instruments with *D* loaded into the sample are significant, and they are much larger than the uncertainty with which lattice parameters can be measured using Rietveld profile analysis on either diffractometer. The distinguishing factor appears to be the temperature and therefore the distance below the critical point at which the isotherm was traversed. We will return to this point in connection with the discussion of Fig. 6.

As a test of the computational approach, the lattice parameter of the "hydride" was measured from the position of the minimum in the formation energy as a function of hydrogen concentration, with hydrogen in *O* sites only, by the lattice relaxation procedure outlined in §*II*.*B*.1. These data are included in Fig. 2. Noting that the DFT calculations are for zero temperature, the difference between the measured lattice parameter of pure Pd at about 300 °C and the DFT prediction agrees well with the measurements of the thermal-expansion coefficient of pure Pd by Nix and MacNair.[41] Noting also that no allowance was made for *T* occupancy in this calculation, the agreement with the trend of the experimental lattice parameters with *D* loaded into the sample is satisfactory. We will return to this point during the discussion of Fig. 7.

B. Interstitial occupancies

Figure 3 shows three sample diffraction profiles, measured on HRPD at ISIS at $T=310$ °C with patterns collected at $D/\mathrm{Pd}=0.22$ [Fig. 3(a)], $D/\mathrm{Pd}=0.28$ [Fig. 3(b)] and

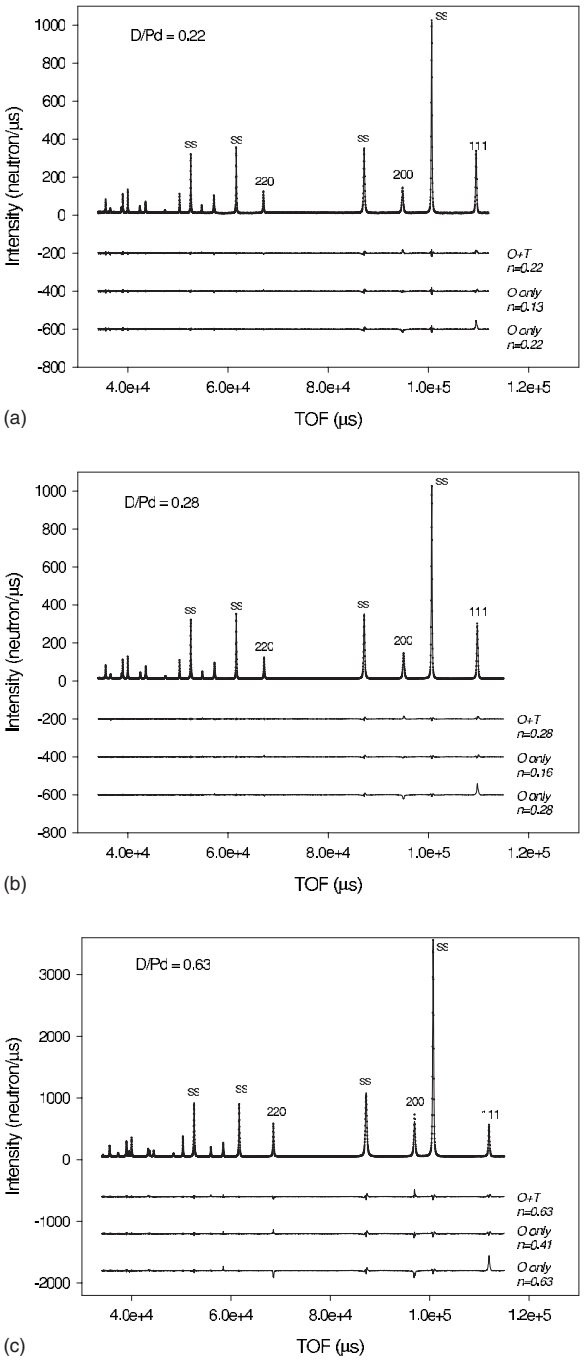

FIG. 3. Results of Rietveld profile analysis of TOF diffraction pattern recorded at (a) $T=310$ °C and $D/M=0.22$, (b) $T=310$ °C and $D/M=0.28$, and (c) $T=310$ °C and $D/M=0.63$. The points are experimental data and the solid line is the fit with a model of combined octahedral and tetrahedral occupancy. The lower lines are difference profiles. Note the misfit to (111) when the pattern is fitted with the *O*-only model with interstitial occupancy fixed at the value corresponding to $D/M=0.28$.

$D/\mathrm{Pd}=0.63$ [Fig. 3(c)]. The fits to the model of simultaneous *O* and *T* occupancy are also shown, along with the difference profiles for fits to the $O+T$ model along with two separate fits using the *O*-only model. In one *O*-only model, the *D* occupancy was fixed to the value corresponding to the manometrically determined value of D/M, while in the other, it

TABLE III. Summary of fit models used on HRPD(ISIS) data.

D/Pd Manometric	$O+T$		O_{free}		O_{fixed}	
	D/Pd	χ^2	D/Pd	χ^2	D/Pd	χ^2
0.22	0.22	1.269	0.13	1.227	0.22	1.384
0.28	0.28	4.586	0.16	3.632	0.28	7.172
0.63	0.63	2.688	0.41	2.469	0.63	7.878

was refined as a separate parameter. Including T occupancy is clearly necessary to obtain an acceptable fit to the (111) peak at the same time as agreement with the manometrically determined D occupancy.

Table III summarizes the results of Fig. 3 including the goodness-of-fit parameter (χ^2) resulting from each Reitfeld refinement. The octahedral-only model fits, where the octahedral occupation number is fixed at the manometrically measured value, have substantially larger (worse) χ^2 values than either of the other two fits. Consistently, the χ^2 obtained from the octahedral-only model where the octahedral occupation number is refined are slightly better than those χ^2 obtained from the octahedral+tetrahedral model, but as they present such a wildly different D/Pd concentration to that measured manometrically they cannot be considered accurate.

The relatively high χ^2 values from the D/Pd=0.28 pattern are possibly an indication that diffraction data present a very slightly two phase pattern. The authors' conclusions regarding the true critical temperature of the palladium-deuterium system will be discussed in a further paper.

Figures 4 and 5 compare the relative heights of low-order peaks as measured from the diffraction profiles and as modeled (Fig. 1). The (111) peak relative to (200) and (220) is consistently higher than can be accounted for by O-only occupancy in the middle range of D concentrations. On the other hand, T occupancy should strongly decrease the (200)/(220) peak height ratio for the fraction of occupied T sites, and the results do indeed show a minimum in this ratio in the middle range of D concentrations. The trends are more obvious on the instrument with superior resolution. As the chief concern is with low-index peaks, the resolution function of a fixed-wavelength powder diffractometer is not optimal, being best at high diffraction angles. In contrast, the TOF instrument has better resolution everywhere, especially at the large d spacings of the low-index Bragg peaks.

Figure 6 shows the interstitial occupancies obtained by Rietveld profile analysis using the $O+T$ model. At the lowest and highest D concentrations, only O sites are occupied. In the middle range of concentrations, however, there is strong evidence for T-site occupancy comparable to the O-site occupancy in the results from the very-high-resolution TOF instrument obtained at the higher temperature of 310 °C. The highest D/M values were achieved by quenching the sample to room temperature under deuterium pressure after reaching the highest achievable D/M at 310 °C. The sample remained single-phase throughout this procedure. The interstitial site occupancies for the quenched samples were obtained by exactly the same analysis procedure as was applied to the diffraction patterns obtained at 310 °C, demonstrating that the much higher tetrahedral occupancy found at high temperatures and lower D concentrations is not an artifact.

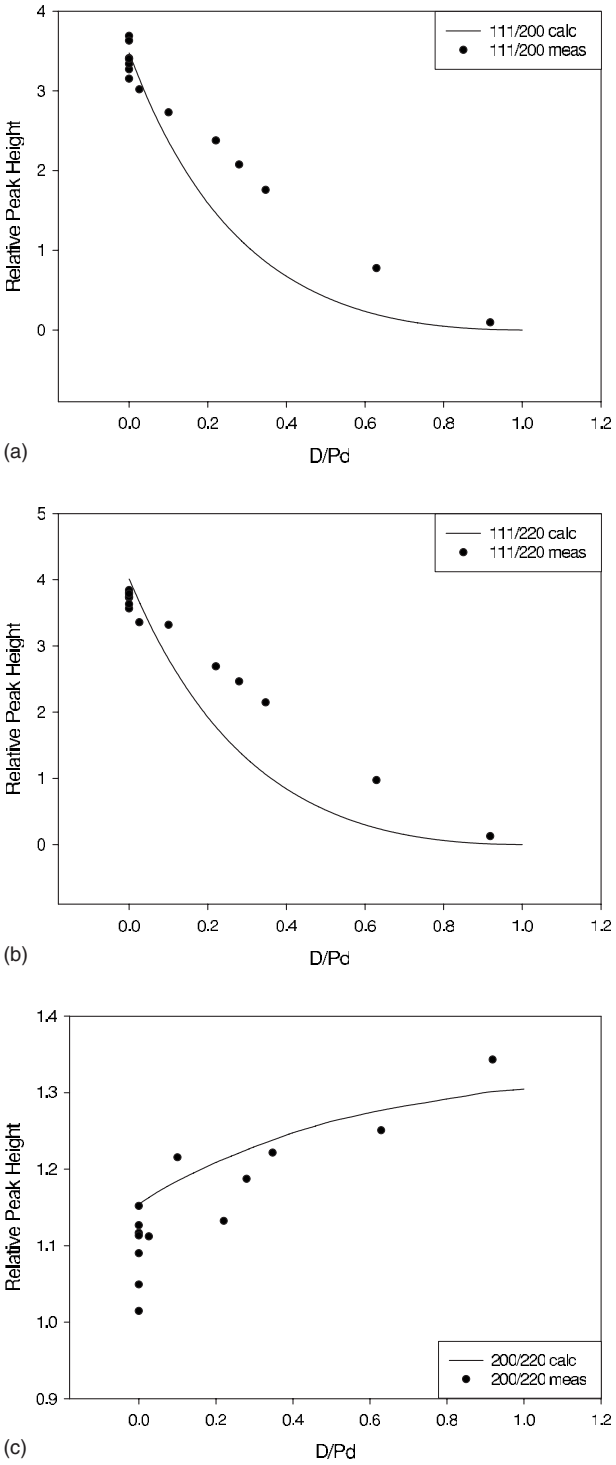

FIG. 4. Relative peak height comparisons for time-of-flight neutron diffractometer. Solid line is calculated for O-only interstitial occupancy model. Points are experimental results from HRPD at ISIS. (a) (111)/(200); (b) (111)/(220); (c) (200)/(220). Note the significant disagreement between the model and experiment in the middle range of D concentrations.

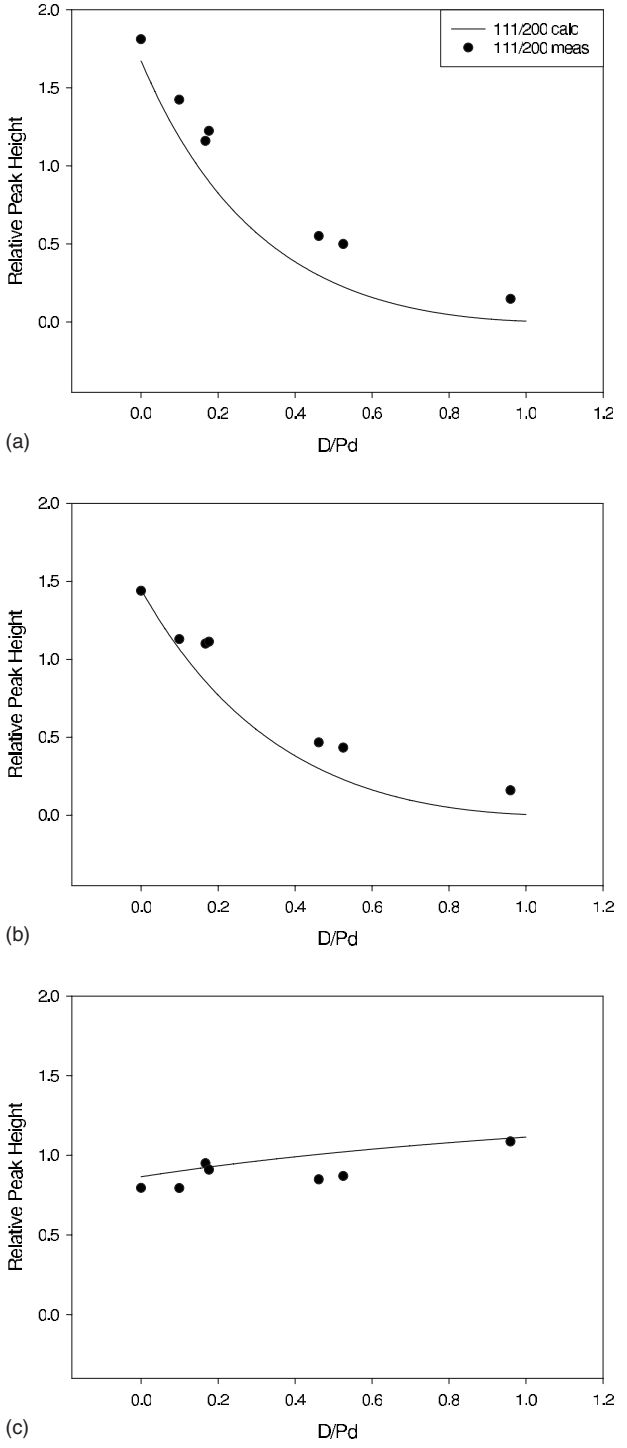

FIG. 5. Relative peak height comparisons for fixed-wavelength diffractometer. Solid line is calculated for *O*-only interstitial occupancy model. Points are experimental results from HRPD at HIFAR. (a) (111)/(200); (b) (111)/(220); (c) (200)/(220). Note the significant disagreement between the model and experiment in the middle range of *D* concentrations.

Given that diffusion between *O* sites occurs via *T* sites, *T*-site occupancy is a question of residence time relative to the time of passage of a neutron, $\sim 10^{-11}$ s for a 1-Å neutron transiting a 1000-Å crystallite of sample. What is surprising is the significantly higher *T* occupancy at the slightly

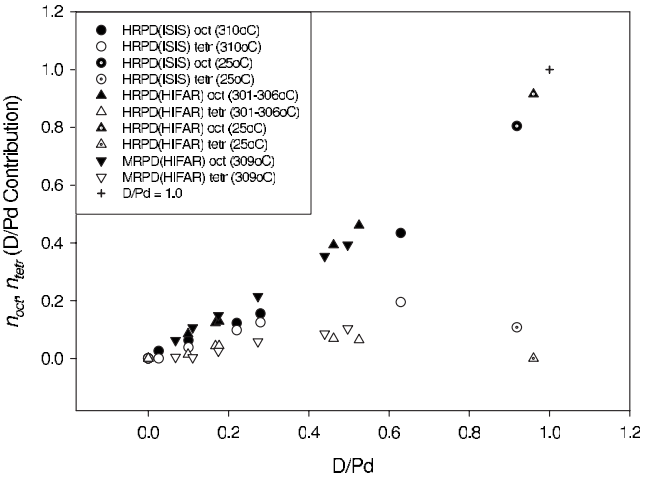

FIG. 6. Deuterium occupancy factors, n_{oct} (filled symbols) and n_{tetr} (open symbols) for *O* and *T* sites from Rietveld refinement of TOF and fixed-wavelength diffraction profiles. $n_{\mathrm{oct}}+n_{\mathrm{tetr}}$ gives the total number of *D* atoms per metal atom. The highest *D* concentrations were achieved by quenching the sample to room temperature through the single-phase (pure β) region. Included for comparison are the data from Ref. 4 (HIFAR MRPD), reanalyzed using the same methodology applied to the data from the two higher-resolution instruments.

higher experimental temperature of 310 °C. This point requires confirmation by measurements in the pericritical region on a single instrument, but is a consistent trend in all the data sets represented in Fig. 6. Longer residence of *D* in the *T* site at higher temperature is counterintuitive unless the occupancy modifies the site by causing the surrounding Pd atoms to relax, as suggested previously[21] and by our calculations presented below.

The trend to maximum *T* occupancy in the middle range of concentrations is understandable in terms of the flux of diffusing atoms, all of which must pass through *T* sites. At low concentrations, there is little diffusive flux, so both the *O* and *T* occupancies are low. At high concentrations, the *O* sites are nearly filled, thus blocking the diffusion pathways. In the middle range of concentrations, therefore, the diffusive flux and potential for *T* occupancy are greatest. There is no evidence to suggest that *T* sites are likely to be occupied when all the *O* sites are filled.

C. Energies of formation

A series of calculations, designed to ascertain the optimal amount of hydrogen in *T* sites, was performed using the doubled unit cell detailed in Sec. II B 1, with all the hydrogen atoms initially in *O* sites. For each hydrogen concentration, theoretical lattice parameters calculated using *O*-only occupancy were used. Owing to the large number of calculations required, the lattice was not relaxed for the repositioning of hydrogen atoms to the tetrahedral positions. A further calculation to validate this constraint is detailed below.

For each concentration, the total energy was calculated as each new configuration replaced *O* with *T* occupancy, one

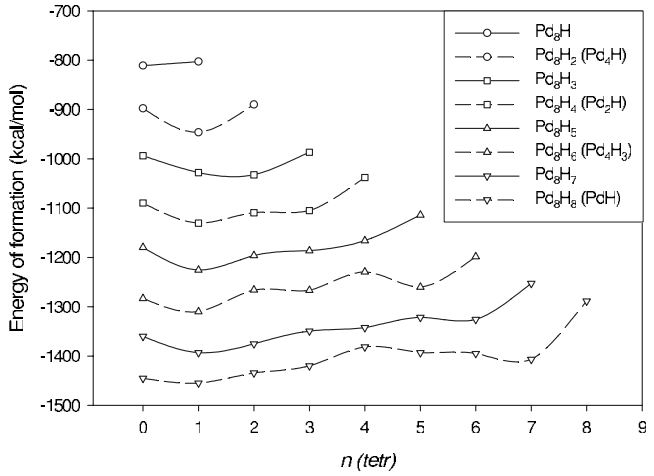

FIG. 7. Calculated energy of formation of PdH_x as a function of *T*-site occupancy, obtained by starting with pure *O* occupancy and progressively moving *H* to *T* sites. *n*(tetr) is the number of hydrogen atoms out of the total in each configuration occupying *T* sites.

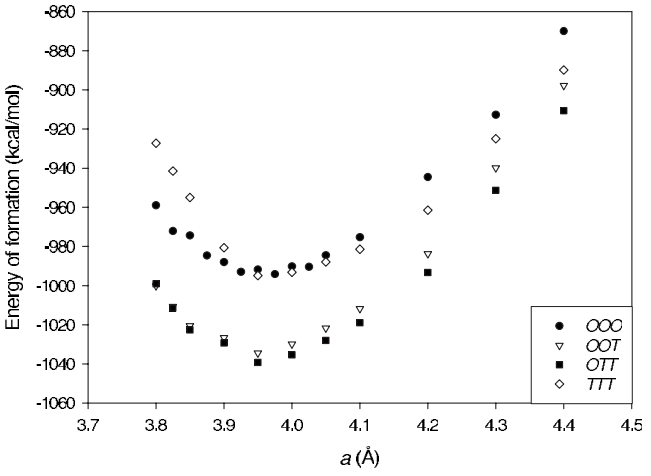

FIG. 8. Energy of formation of Pd_8H_3, calculated with lattice relaxation, for the possible interstitial configurations. Note the lower formation energy with one or two occupied *T* sites.

atom at a time, until all *O* sites were converted to *T* sites. Owing to the large number of cases to be computed (44), these calculations were performed using only three wave vectors, a relatively low accuracy though accurate enough to indicate general trends. The doubled unit cell containing eight Pd atoms was used for all calculations. Figure 7 shows the results. It is apparent that there is a preference for one hydrogen atom to occupy a *T* site, except in the cases of Pd_8H, where the hydrogen atom prefers the *O* position, and Pd_8H_3, where two hydrogen atoms preferentially occupy *T* sites.

O and *T* site occupation in Pd_8H_3 was also studied with lattice relaxation permitted. The total energy of formation was calculated for each hydrogen configuration [(*OOO*), (*TOO*), (*TTO*), (*TTT*)] for a range of lattice constants about the experimental value. These results are shown in Fig. 8.

In Fig. 8, the unit-cell volume is adjusted to minimize the energy at each configuration of the hydrogen. Possible further distortions of the Pd lattice within the unit cell are not considered here. Neither is the change in hydrogen vibrational zero-point energy at the *T* site compared to that at the *O* site. In fact, the work of Elsässer *et al.*[27,31] shows, in a determination of the energy cost to have a *H* atom at the *T* site rather than the *O* site, that these effects tend to cancel. Specifically, the energy cost of moving *H* from an *O* site to a *T* site is lowered by static Pd lattice distortion.[31] On the other hand, the *H* zero-point vibrational energy is increased at the *T* site, compared with the *O* site, which raises the energy cost of moving from *O* to *T*. We therefore expect that the present calculations of the energy as a function of the occupation of the *T* site (Fig. 7) will be at least qualitatively correct.

There is a clear preference for one or two hydrogen atoms in tetrahedral sites, consistent with the unrelaxed calculation of this stoichiometry (Fig. 7). The small variation of the minimum-energy lattice parameter over the four interstitial configurations in Fig. 8 relative to the scatter in the formation energy suggests that the calculations performed without lattice relaxation are valid, at least as far as estimating the optimal mix of *O*-site and *T*-site occupancy is concerned.

Figure 8 shows that the formation energy rises more steeply with lattice compression as the fraction of *T* sites occupied in Pd_8H_3 rises. This is consistent with the closer proximity of Pd atoms surrounding the *T* sites relative to the *O* sites.

While the DFT calculations predict *T* occupancy at zero temperature in a single-phase sample, this condition is never realized, except at very low and very high concentrations of *H*, as the system becomes two phase in the miscibility gap below its critical point at around 300 °C.

Returning to the dependency of the lattice parameter on the detailed interstitial site occupancy, Fig. 8 reveals a slight displacement to lower values with 1 or 2 *D* in *T* sites, amounting to around 0.01 Å. This feature requires confirmation by more detailed calculations, but is consistent with the trend in Fig. 6 to lower lattice parameter in the measurements that revealed higher *T* occupancy, for those performed at 310 °C. The interesting possibility is thus raised that *T* occupancy actually lowers the lattice parameter. The rapid dependence of both lattice parameter (Fig. 2) and site occupancy (Fig. 6) on temperature just below the critical point suggests that *T* occupancy is an important feature of the pericritical region itself, whether as a determining factor or a consequence we cannot yet say.

IV. CONCLUSIONS

Occupation by deuterium of the interstitial sites in palladium has been studied by the neutron powder diffraction at the highest available resolution on single-phase samples, and by DFT-based calculations of formation energies. Both approaches indicate significant *T*-site occupancy in the middle range of *D* concentrations.

The experimental evidence was gained from Rietveld profile analysis of diffraction patterns from two diffractometers, based on independent knowledge of the deuterium concentration in the sample. The (111) Bragg peak could not be fitted with an octahedral-only occupancy model. Further-

more, the measured relative intensities of the three lowest-order Bragg peaks [(111), (200), and (220)] as functions of D concentration did not agree with the calculated effects of octahedral-only occupancy.

Calculations of the formation energy of numerous Pd_mD_n pseudostoichiometries showed that hydrogen prefers to occupy some of the available tetrahedral sites, particularly in the middle range of concentrations around Pd_8H_4. Our computational technique was tested by calculating the single-phase lattice parameter/concentration relationship, with results that agreed with experiment to within the uncertainty of the calculation.

ACKNOWLEDGMENTS

The authors thank M. P. Pitt for helpful discussions and original data from Ref. 4, and K. S. Knight for assistance with the neutron-diffraction measurements at ISIS. This work was supported by the Australian Research Council, The Australian Institute of Nuclear Science and Engineering and the Access to Major Research Facilities Program.

*Corresponding author: CSIRO Energy Technology, QCAT, GPO Box 883, Kenmore QLD 4069, Australia; keith.mclennan@csiro.au; Tel.: +61 7 3327 4127; Fax: +61 7 3327 4455;

†Present address: CSIRO Energy Technology, QCAT, Pullenvale 4069, Australia.

[1] Generally we use "hydrogen" to denote any of the isotopes $^1_1$H (protium, symbol H), $^2_1$H (deuterium, symbol D) or $^3_1$H (tritium, symbol T). Where necessary we refer explicitly to the isotope by its name or symbol.

[2] B. Baranowski and R. Wisniewski, Phys. Status Solidi **35**, 593 (1969).

[3] E. Wicke and J. Blaurock, J. Less-Common Met. **130**, 351 (1987).

[4] M. P. Pitt and E.MacA. Gray, Europhys. Lett. **64**, 344 (2003).

[5] L. W. McKeehan, Phys. Rev. **21**, 334 (1923).

[6] A. J. Maeland and T. R. P. Gibbs, Jr., J. Phys. Chem. **65**, 1270 (1961).

[7] J. E. Worsham, M. K. Wlkinson, and C. G. Shull, J. Phys. Chem. Solids **3**, 303 (1957).

[8] J. Bergsma and J. A. Goedkoop, Physica (Amsterdam) **26**, 744 (1960).

[9] G. A. Ferguson, A. J. Schindler, T. Tanaka, and T. Morita, Phys. Rev. **137**, A483 (1965).

[10] M. M. Beg and D. K. Ross, J. Phys. C **3**, 2487 (1970).

[11] G. Nelin, Phys. Status Solidi **45**, 527 (1971).

[12] I. R. Entin, V. A. Somenkov, Ya. S. Umanskii, A. A. Chertkov, and S. S. Shilstein, Sov. Phys. Solid State **15**, 1840 (1974).

[13] M. H. Mueller, J. Faber, H. E. Flotow, and D. G. Westlake, Acta Crystallogr., Sect. A: Cryst. Phys., Diffr., Theor. Gen. Crystallogr. **31**, S99 (1975).

[14] I. S. Anderson, D. K. Ross, and C. J. Carlile, Phys. Lett. **68A**, 249 (1978).

[15] I. S. Anderson, C. J. Carlile, and D. K. Ross, J. Phys. C **11**, L381 (1978).

[16] O. Blaschko, R. Klemencic, P. Weinzierl, and O. Eder, Solid State Commun. **27**, 1149 (1978).

[17] T. E. Ellis, C. B. Satterthwaite, M. H. Mueller, and T. O. Brun, Phys. Rev. Lett. **42**, 456 (1979).

[18] O. Blaschko, R. Klemencic, P. Weinzierl, and O. Eder, J. Phys. F: Met. Phys. **9**, L113 (1979).

[19] O. Blaschko, R. Klemencic, P. Weinzierl, O. Eder, and P. von Blanckenhagen, Acta Crystallogr., Sect. A: Cryst. Phys., Diffr., Theor. Gen. Crystallogr. **36**, 605 (1980).

[20] O. Blaschko, P. Fratzl, and R. Klemencic, Phys. Rev. B **24**, 277 (1981).

[21] D. K. Ross, M. W. McKergow, D. G. Witchell, and J. K. Kjems, J. Less-Common Met. **172-174**, 169 (1991).

[22] A. C. Lawson, J. W. Conant, R. Robertson, R. Rohwer, V. A. Young, and C. L. Talcott, J. Alloys Compd. **183**, 174 (1992).

[23] E. Wu, S. J. Kennedy, E. H. Kisi, and E. Mac A. Gray, J. Alloys Compd. **231**, 108 (1995).

[24] S. J. Kennedy, E. Wu, E. H. Kisi, E. Mac A. Gray, and B. J. Kennedy, J. Phys.: Condens. Matter **7**, L33 (1995).

[25] E. Wu, S. J. Kennedy, E. Mac A. Gray, and E. H. Kisi, J. Phys.: Condens. Matter **8**, 2807 (1996).

[26] C. Elsässer, M. Fahnle, K. M. Ho, and C. T. Chan, Physica B (Amsterdam) **172**, 217 (1991).

[27] C. Elsässer, K. M. Ho, C. T. Chan, and M. Fähnle, Phys. Rev. B **44**, 10377 (1991).

[28] C. Elsässer, K. M. Ho, C. T. Chan, and M. Fähnle, J. Phys.: Condens. Matter **4**, 5207 (1992).

[29] C. Elsässer, M. Fahnle, L. Schimmele, C. T. Chan, and K. M. Ho, Phys. Rev. B **50**, 5155 (1994).

[30] K. M. Ho, C. Elsässer, C. T. Chan, and M. Fähnle, J. Phys.: Condens. Matter **4**, 5189 (1992).

[31] H. Krimmel, L. Schimmele, C. Elsässer, and M. Fähnle, J. Phys.: Condens. Matter **6**, 7679 (1994).

[32] Amsterdam Density Functional program (http://www.scm.com/).

[33] L. Koester, H. Rauch, and E. Seymann, At. Data Nucl. Data Tables **49**, 65 (1991).

[34] *International Tables for Crystallography*, edited by U. Shmueli (Kluwer, Dordrecht, 1993), Vol. B, p. 152.

[35] B. A. Hunter, Commission on Powder Diffraction Newsletter **20**, 21 (1998).

[36] http://www.isis.rl.ac.uk/crystallography/hrpd/

[37] http://www.ansto.gov.au/ansto/bragg/hifar/hrpd.html

[38] K. G. McLennan and E. Mac A. Gray, Meas. Sci. Technol. **15**, 211 (2004).

[39] F. M. Mueller, A. J. Freeman, J. O. Dimmock, and A. M. Furdyna, Phys. Rev. B **1**, 4617 (1970).

[40] J. P. Perdew, J. A. Chevary, S. H. Vosko, K. A. Jackson, M. R. Pederson, D. J. Singh, and C. Fiolhais, Phys. Rev. B **46**, 6671 (1992).

[41] F. C. Nix and D. MacNair, Phys. Rev. **61**, 74 (1941).